

# Morphology and elastomeric properties of isotactic polypropylene/hydrogenated poly(styrene-*co*-butadiene) blends: a potential for a new thermoplastic elastomer

Ying Yang<sup>a</sup>, Nobuyoshi Otsuka<sup>a</sup>, Hiromu Saito<sup>a</sup>, Takashi Inoue<sup>a,\*</sup>, Yasuhiko Takemura<sup>b</sup>

<sup>a</sup>Department of Organic and Polymeric Materials, Tokyo Institute of Technology, Ookayama, Meguro-ku, Tokyo 152, Japan

<sup>b</sup>TPE Laboratory, JSR Co. Ltd, 100 Kawajiri, Yokkaichi 510, Japan

Received 29 January 1998; revised 15 April 1998; accepted 30 April 1998

## Abstract

A single-phase melt of the isotactic polypropylene (iPP)/hydrogenated poly(styrene-*co*-butadiene) (hSBR) blend, which has a virtual upper critical solution temperature (UCST)-type phase boundary below the melting point of iPP ( $T_m$ ), was prepared at 50/50 wt. ratio and quenched below UCST. By transmission electron microscopy and dynamic mechanical analysis, the blend was shown to be a phase-separated material in which hSBR-rich domains with uniform diameter of ca. 20 nm are dispersed in an iPP-rich matrix. The regular structure is believed to be formed by spinodal decomposition which is pinned at an early stage by crystallization in the iPP-rich region. The blend showed good strain recovery after large deformation, suggesting a potential for a new class of thermoplastic elastomer. Wide-angle X-ray diffraction (WAXD) studies showed that iPP crystallites in the blend are smaller than those in neat iPP and there exists an optimum size of ca. 10 nm (crystal size by the Scherrer equation) for this strain recovery. Such crystallites suffered from less plastic deformation and were hardly oriented under bulk deformation. That is, the crystallites that developed in the presence of polymer impurity (hSBR) seem to be different from those in neat iPP, and play the role of tie points to provide the elastomeric character of the matrix itself. © 1998 Elsevier Science Ltd. All rights reserved.

**Keywords:** Polypropylene; Hydrogenated poly(styrene-*co*-butadiene); Blend

## 1. Introduction

Most pairs of high molar mass polymers are immiscible. This is so because the combinatorial entropy of mixing of the two polymers is dramatically less than that for the corresponding two low mass compounds. However, several combinations of dissimilar polymers have been found to follow a phase diagram; i.e., the polymers are miscible over a limited temperature and composition range but are immiscible outside this range. Such phase behaviour is called LCST (lower critical solution temperature)-type and UCST (upper critical solution temperature)-type [1].

We recently found that isotactic polypropylene (iPP) is miscible with a hydrogenated poly(styrene-*co*-butadiene) (hSBR) above the melting point ( $T_m$ ) of iPP and that the blend shows virtual UCST-type phase behaviour [2]. The phase diagram is reproduced in Fig. 1. The UCST phase boundary was determined by kinetic analysis of crystallization below  $T_m$  using time-resolved light scattering, i.e. by a

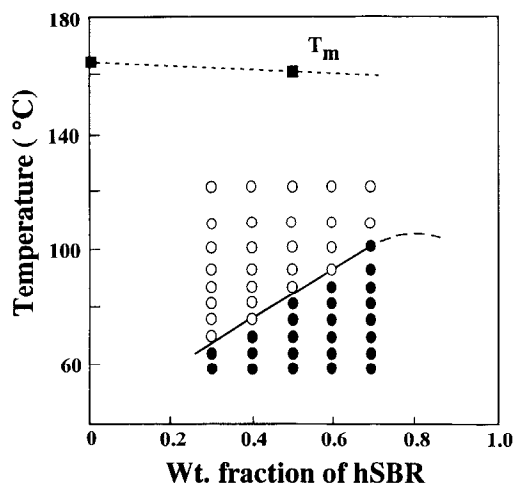


Fig. 1. Phase diagram of iPP/hSBR blend [2]. A virtual UCST phase boundary was determined by a discontinuity in temperature dependence of crystallization rate [3,4]. Data points below and above the discontinuity are presented by closed and open circles, respectively.

\* Corresponding author.

discontinuity in the temperature dependence of the crystallization rate at UCST, as in other virtual UCST systems [3,4].

For the UCST system in Fig. 1, one can expect a variety in morphology development. If the single-phase mixture prepared above  $T_m$  undergoes a temperature drop to a temperature below  $T_m$  and above UCST, the crystallization takes place in the presence of polymer impurity (hSBR). If the temperature drops to below UCST, spinodal decomposition will proceed and will compete with the crystallization. In this paper, we pay attention just to the latter process. We quench the single-phase mixture below UCST, investigate the structure by transmission electron microscopy, dynamic mechanical analysis and wide-angle X-ray diffraction, and measure the mechanical properties. Then the structure–property relationship will be discussed, paying attention especially to the elastomeric property of the quenched blend.

## 2. Experimental

The polymers used in this work were isotactic polypropylene (iPP) supplied by Mitsui Toatsu Chemicals Inc. (J3HG,  $M_w = 3.5 \times 10^5$  and  $M_n = 5 \times 10^4$ ) and a hydrogenated poly(styrene-*co*-butadiene) from JSR Co. Ltd (Dynaron 1320P,  $M_w = 3 \times 10^5$ , styrene content = 10 wt%).

A 50/50 (wt. ratio) blend of iPP/hSBR was prepared by melt mixing in a miniature mixer (Mini-Max Molder, Model CS-183 MMX, Custom Scientific Instruments Inc.) at 210°C for 5 min. The melt-mixed blend was extruded and compression moulded to a thin sheet of 2 mm thickness at 200°C. The moulded sheet was quenched in various ways: quenching in water, ice and dry ice–acetone ( $\sim -60^\circ\text{C}$ ). The quenched samples were coded as W, I and D, respectively. To obtain a highly crystallized sample, the blend quenched in water was further isothermally annealed at 140°C for 80 min, then quenched in water (coded as QA). Neat iPP specimens with the same thermal treatment conditions as above were also prepared as control samples.

The tensile stress–strain curve at room temperature was obtained with a tensile testing machine (Tensilon UTM-II-20, Toyo Baldwin Co. Ltd) with a crosshead speed of 10 mm min<sup>-1</sup>. After the preset strain was attained the crosshead returned at the same speed as when stretching. After the strain reached zero, the sample was released from the clamps and the residual strain was measured at certain intervals.

Dynamic mechanical behaviour was measured with a Toyoseiki Dynamic Mechanical Analyzer at 100 kHz at a heating rate of 2°C min<sup>-1</sup>. Temperature dependence of the dynamic loss ( $\tan \delta$ ) was obtained.

For transmission electron microscope (TEM) observation, the specimen was stained with ruthenium tetroxide (RuO<sub>4</sub>) vapour for 0.5 h at 50°C. The stained specimen

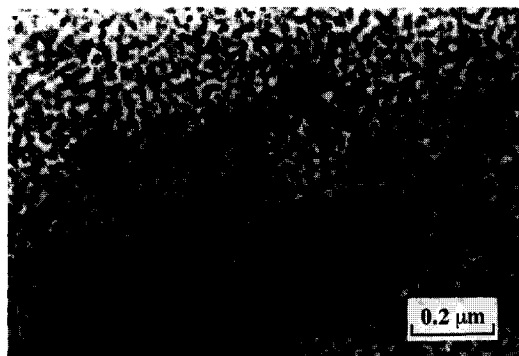


Fig. 2. TEM micrograph of the blend quenched in water.

was microtomed to obtain ultrathin sections of ca. 70 nm thickness using an ultra-cryomicrotome, Ultracut N, Reichert–Nissei, at  $-70^\circ\text{C}$ . The structure in the section was observed with a JEOL electron microscope, JEM-100CX.

Wide angle X-ray diffraction (WAXD) was measured in a Rigaku Denki Ru-200 X-ray diffraction apparatus using image plate RAXIS II D. Cu anode radiation was reflected from a graphite monochromator to obtain monochromatic Cu K $\alpha$  radiation with a wavelength of 0.1541 nm. The generator was operated at 40 kV and 100 mA.

## 3. Results and discussion

Fig. 2 is a TEM micrograph of the blend quenched in water (blend W). The dark domains with a uniform diameter of ca. 20 nm are dispersed fairly regularly in a bright matrix. These dark domains can be assigned to an hSBR-rich phase since the styrene unit is reactive with RuO<sub>4</sub>. Similar morphology was observed for the blends quenched under other conditions (blends I and D).<sup>1</sup>

The regularly phase-separated structure in Fig. 2 could not be attained by simple melt mixing of an immiscible system. Following the phase diagram in Fig. 1, the regular structure may be formed by spinodal decomposition on quenching into water, i.e. by the temperature dropping below UCST, and the decomposed structure could be fixed at a relatively early stage by the crystallization of iPP which prevents the further interdiffusion of component molecules. It is interesting to note that the ratio of bright to dark areas in Fig. 2 is ca. 70/30, far from the charge ratio of 50/50. This suggests that part of the hSBR may reside in the matrix as a mixture with iPP. To discuss this point, one should consider the glass transition temperature ( $T_g$ ) behaviour of the blend.

<sup>1</sup> This implies that crystallization and spinodal decomposition could take place (as will be discussed later) even by quenching near or below  $T_g$ . Such a phase transition may occur mostly during cooling in a finite time interval (due to the poor heat conductivity of polymers) before the low temperature is attained.

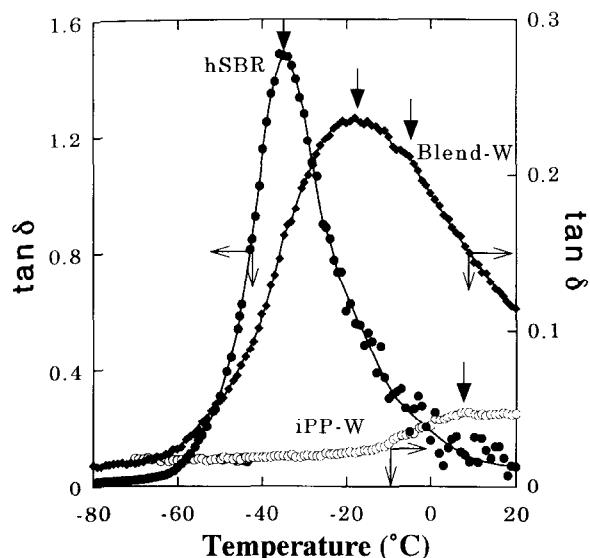


Fig. 3. Dynamic loss versus temperature curves for neat iPP, hSBR and the blend. All specimens were melt-pressed at 210°C and quenched in water.

Fig. 3 shows the temperature dependence of the dynamic loss for the component polymers and the blend quenched in water (blend W). There are two  $\tan \delta$  peaks (two  $T_g$ s) in the blend, as indicated by the arrows, and both peaks shift inward in comparison with those of the neat polymers, indicating a phase-separated state in which both phases are not pure but are mixtures, i.e. iPP-rich and hSBR-rich mixtures. This implies that the spinodal decomposition, after quenching in water, was pinned by the crystallization of iPP at a relatively early stage to yield the regularly arranged hSBR-rich domains dispersed in an iPP-rich matrix. Thus the ratio of dark and bright areas in Fig. 2 could be different from the charge ratio of 50/50.

In Fig. 4 is shown a TEM micrograph of the blend quenched in water and then annealed at 140°C (blend QA). The hSBR-rich domains are still dispersed in the iPP-rich matrix, but they are somewhat clustered in comparison with Fig. 2. This may suggest that the arrangement of the hSBR domains is slightly affected by the



Fig. 4. TEM micrograph of the quenched and annealed blend.

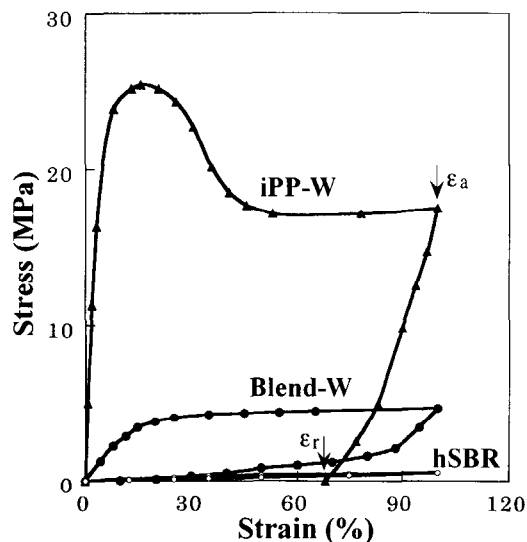


Fig. 5. Typical stress-strain curves for the blend and component polymers.

crystallization of iPP during annealing at 140°C ( $< T_m$  of iPP). Loci of individual hSBR domains could be changed by a supply of crystallizable moiety (iPP chains) from matrix to crystal growth front and by a segregation of impurity (hBR) from crystals. The crystallization will be discussed later in terms of WAXD results.

Typical stress-strain curves are shown in Fig. 5. Neat iPP shows large residual strain, which is natural for the ductile thermoplastic. In contrast, good strain recovery is seen for the blend quenched in water (blend W). This is an interesting behaviour: even though the matrix is the iPP-rich phase, the two-phase material can shrink back from a highly deformed state. That is, the quenched blend behaves like a vulcanized rubber at ambient temperature. It is actually a thermoplastic elastomer (TPE); i.e., the melt-processed and quenched blend shows good elastomeric behaviour.

There are two groups of TPEs [5]. The first consists of styrene–diene block copolymers, polyether–ester multi-block copolymers and segmented polyurethanes. Another class of TPEs is prepared by dynamic vulcanization of iPP and ethylene–propylene–diene rubber (EPDM). The result in Fig. 5 implies a potential for the development of a third class of TPEs prepared by simple melt mixing. However, the question turns on the strain recovery behaviour of iPP/hSBR blends; i.e., why the blend can shrink back from the highly deformed state even though the matrix mostly consists of ductile polymer (iPP), as shown in Fig. 2. The question may be similar to one relating to iPP/EPDM TPE [6,7]. However, in the present case, the hSBR domains are not crosslinked. A key to understanding the recovery mechanism may reside in the crystalline structure of the iPP-rich matrix. Actually, the strain recovery depends on the crystal size, as shown below.

Good strain recovery behaviour was observed also for the other blends subjected to various heat treatments (blends I, D and QA). The residual strain decreased with time after the

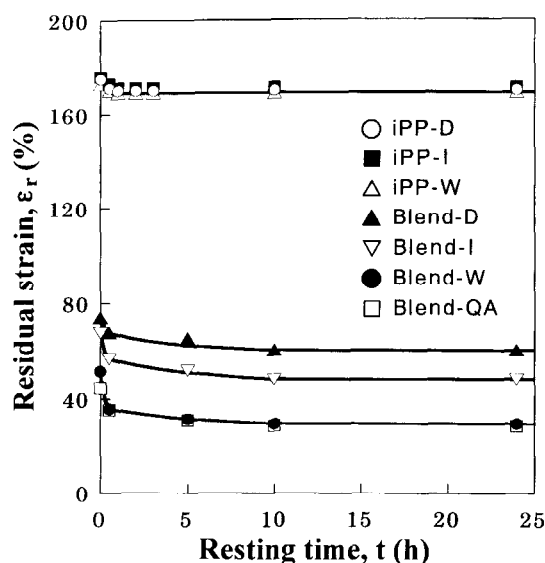


Fig. 6. Residual strain after release from 200% elongation as a function of resting time for neat iPP and for blends with different thermal treatments.

sample was released from clamps. The time variation of residual strain is shown in Fig. 6. Residual strain levels off at ca. 1 h of resting. The levelled-off residual strain is shown as a function of applied strain in Fig. 7. One sees a big difference in strain recovery behaviour between neat iPP and the blends. There is also a small but definite difference in strain recovery between the blends. This difference could be caused by the different thermal treatments which would affect crystalline structure in the iPP-rich matrix. The presence of impurity, hSBR in this system, could affect the crystallization of iPP to yield a different morphology from neat iPP [8–10]. The investigation of crystalline structure is

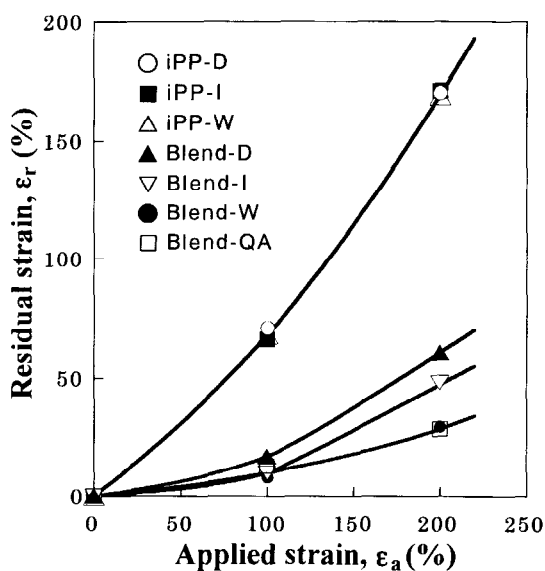


Fig. 7. Residual strain versus applied strain for the same specimens as in Fig. 6.

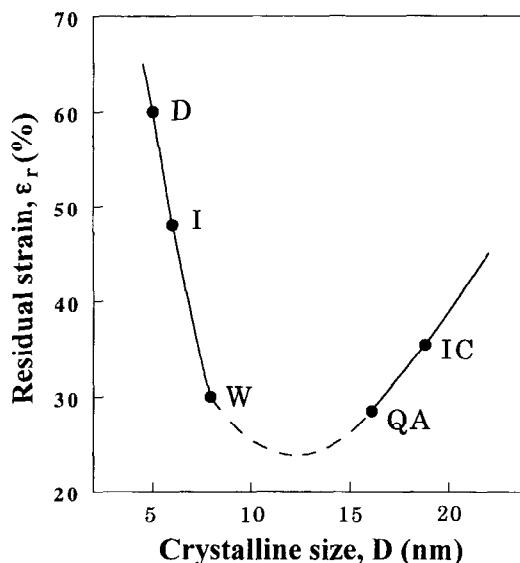


Fig. 8. Residual strain after 200% elongation versus iPP crystalline size in the blends. A sample coded as IC was prepared by isothermal annealing at 140°C for 12 h to obtain crystallites with higher ordering.

expected to lead to a proper understanding of the strain recovery mechanism.

From WAXD profiles (see Figs 9 and 10), the apparent crystal size (*D*) in the perpendicular direction to the [110] plane ( $2\theta = 14.16^\circ$ ) was calculated by the Scherrer equation. As shown in Fig. 8, the lower the quenching temperature (water [W] > ice [I] > dry ice–acetone[D]), the smaller was the crystal size, and the size increased with annealing at high temperatures. In Fig. 8, the levelled-off residual strain after 200% elongation is plotted as a function of the crystal size. One can see that there exists an optimum crystalline size which provides the best strain recovery.

As shown in Table 1, the crystals in the blends are smaller than those in neat iPP subjected to the same thermal treatment. The hSBR, which had remained in the matrix, may act as a polymer impurity to reduce the crystal size. The physical meaning of crystal size by the Scherrer equation is not fully understood and one cannot discuss quantitatively the size of crystallites. However, a smaller size according to the Scherrer equation may imply more disordered crystallites. In the extreme case, the crystallite could consist of fragmented lamellae as in the case of iPP/oligomer blend [10]. In fact, there are no visible lamellae in TEM in Figs 2 and 4. The fragmented lamellae could act as tie points to provide high strain recovery. If the crystallites are

Table 1  
Apparent crystal size (*D*/nm) perpendicular to the [110] plane

	W	QA	IC
iPP	11.7	16.5	21.2
Blend	7.9	16.1	18.8

W: quenched in water; QA: quenched in water and annealed at 140°C; IC: isothermally crystallized at 140°C.

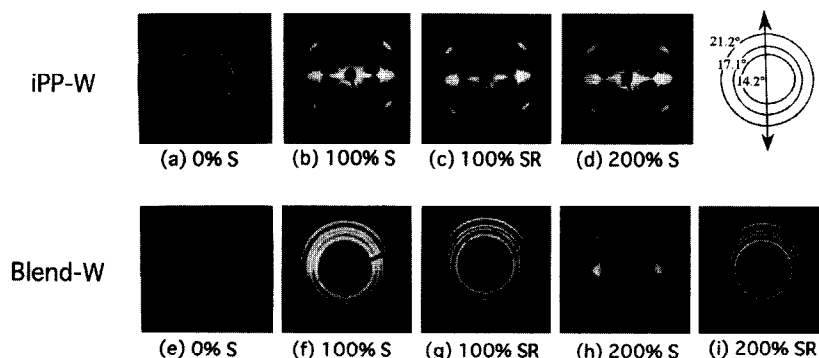


Fig. 9. Change of WAXD pattern with bulk deformation for neat iPP (a–d) and for the blend quenched in water (e–i). S: stretched state; SR: stretched-and-released state. Number indicates percentage elongation. The stretching direction is vertical, as shown by the arrow.

fragmented too much (e.g., yielding smectic crystals [11]), the small crystallites can be easily destroyed or plastically deformed under stress evolved by bulk deformation and then cannot be the tie points to render poor strain recovery. Thus there should exist an optimum crystal size. Such a scenario may be supported by the WAXD studies on deformation, as follows.

The change of WAXD pattern with bulk deformation for neat iPP is shown in Fig. 9(a–d). At 100% elongation, the crystallites in neat iPP intensively orient in the stretching direction, as shown by the appearance of three bright arcs in the equator and four arcs in the diagonal direction (b), and the orientation never recovers after the sample is released from clamps (c). At high elongation, the arcs become shorter and brighter (d). The results suggest a plastic deformation of the crystallites. This is the typical orientation behaviour of crystalline polymers. The results for blend W are shown in Fig. 9(e–i). One can see that the crystal orientation is negligible; compare (e) (undeformed) with (f) (100% elongation). At 200% elongation, short arcs appear in the equator (h) but disappear after release (i). Comparing with the results for neat iPP, one sees that iPP crystallites in the blend hardly orient with bulk deformation and show better recovery after release of the bulk strain.

Similar results are shown for blend QA in Fig. 10(a–e). It is surprising that crystal orientation is not seen even at 200%

elongation. In contrast, crystal orientation takes place in blend D (g, i) and hardly recovers after release (h, j). The small and disordered crystallites in blend D seem to be destroyed or remelted by the bulk deformation to form new crystallites oriented preferentially in the stretching direction. In such a way, the small crystallites cannot play the role of tie points for strain recovery.

The results shown in Fig. 10(a–e) are interesting. At present, one cannot provide a proper explanation for the non-orientation of iPP crystallites in blend QA. However, there might exist a situation in which fragmented crystallites of appropriate size are resistant to rotation or orientation with bulk deformation and will consequently act as tie points for strain recovery. Such a situation may be created by crystallization in the presence of high molecular impurity (hSBR).

The crystal orientation and its recovery can be discussed more quantitatively in terms of the crystal orientation function,  $f$ . The value of  $f$  was estimated by Wilchinsky's method [12] using [110] ( $2\theta = 17.08^\circ$ ) and [040] ( $2\theta = 14.16^\circ$ ) diffractions, because in the case of monoclinic iPP there is no set of diffracting [001] planes which reveals orientation of the  $c$ -axis directly; thus, the diffraction from two sets of planes containing the  $c$ -axis, such as [110] and [040], could be used to calculate the average orientation of the  $c$ -axis. The estimated orientation function is shown as a function of the applied strain in both the as-stretched state

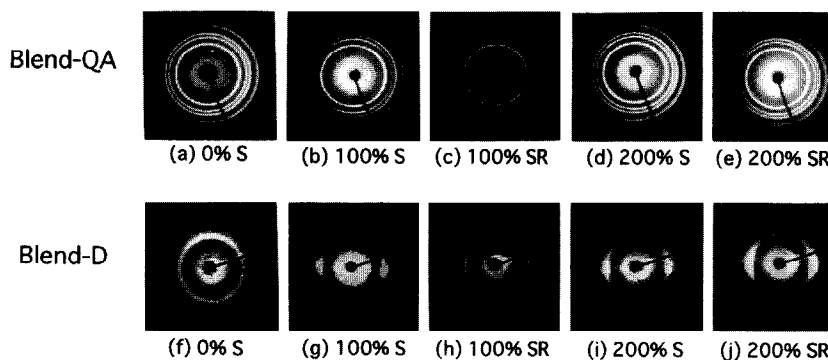


Fig. 10. Change of WAXD pattern with bulk deformation for the blends with different thermal treatments. (a–e): quenched and annealed; (f–j): quenched in dry ice–acetone. S: stretched state; SR: stretched-and-released state. Number indicates percentage elongation.

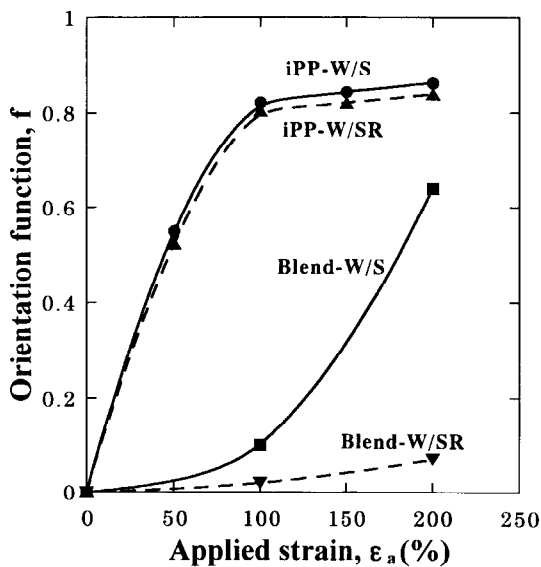


Fig. 11. Orientation function versus applied strain for the blend quenched in water. S: stretched state; SR: stretched-and-released state.

(symbol S) and the stretched-and-released state (SR) in Fig. 11. One sees a big difference in  $f$  between neat iPP and blend W, especially in the released state. The results suggest again that the iPP crystallites in the blend hardly orient with bulk deformation and that the orientation relaxes better on release.

#### 4. Conclusion

Melt blending of iPP with hSBR yields a phase-separated material in which hSBR-rich domains with a uniform diameter of 20 nm are dispersed in an iPP-rich matrix.

The regular structure seems to be formed by spinodal decomposition. The blend shows good strain recovery after large deformation, suggesting a potential for a new class of TPE. The presence of rubbery (hSBR-rich) domains may provide a favourable contribution to the good strain recovery mechanism, as we have discussed for TPE made by dynamic vulcanization in terms of elastic–plastic analysis using the finite element method [7,8]. The strain recovery mechanism may also originate from the characteristic morphology of iPP crystallites in the matrix; i.e., rather fragmented crystallites formed by crystallization in the presence of polymer impurity (hSBR). That is, the matrix itself is expected to be less ductile and much more elastomeric than neat iPP. An optimum crystal size for good strain recovery was found to exist.

#### References

- [1] Olabishi O, Robeson LM, Show MT. Polymer–polymer miscibility. New York: Academic Press, 1979.
- [2] Otsuka N, Yang Y, Saito H, Inoue T, Takemura Y. Polymer 1998;39:1533.
- [3] Tomura H, Saito H, Inoue T. Macromolecules 1992;25:1611.
- [4] Svoboda P, Kressler J, Chiba T, Inoue T, Kammer HW. Macromolecules 1994;27:1154.
- [5] Bhomwick AK, Stephens HL, editors. Handbook of elastomers—new development and technology. New York: Marcel Dekker, 1988.
- [6] Kikuchi Y, Fukui T, Okada T, Inoue T. Polym Eng Sci 1991;31:1029.
- [7] Okamoto M, Shiomi K, Inoue T. Polymer 1994;35:4618.
- [8] Karger-Kocsis J, Kallo A, Szafiner A, Bodor G, Senyei Z. Polymer 1979;20:37.
- [9] D'orazio L, Mancarella C, Martuscelli E, Sticotti G, Ghisellini R. J Appl Polym Sci 1994;53:3873.
- [10] Lee CH, Saito H, Inoue T. Macromolecules 1995;28:8096.
- [11] Vittoria V. J Macromol Sci Phys 1989;B28:489.
- [12] Wilchinsky ZW. J Appl Phys 1960;3:1969.